

Dispersive atom-field interaction scheme for three-dimensional entanglement between two spatially separated atoms

Xin-You Lü,^{1,*} Ji-Bing Liu,^{2,1} Chun-Ling Ding,¹ and J.-H. Li¹

¹Wuhan National Laboratory for Optoelectronics and School of Physics, Huazhong University of Science and Technology, Wuhan 430074, People's Republic of China

²Department of Physics, Hubei Normal University, Huangshi 435002, People's Republic of China

(Received 19 June 2008; published 3 September 2008)

We propose a scheme for deterministically generating three-dimensional (3D) entanglement between two distant five-level atoms based on the dispersive atom-field interaction. In our scheme, the two atoms are trapped separately in two spatially separated optical cavities coupled by an optical fiber. To check the experimental feasibility of our scheme, we numerically simulated effects of the atomic spontaneous decay and photon leakage out of the fiber, and the numerical simulation shows that those effects can be suppressed by appropriately choosing the frequency detuning of atom-field and the coupling intensity of cavity fiber, respectively. We also discussed the influence of photon leakage out of the cavities, and the strictly numerical simulation shows our proposal is good enough to demonstrate the generation of 3D entanglement with high fidelity and within the current experimental technology.

DOI: [10.1103/PhysRevA.78.032305](https://doi.org/10.1103/PhysRevA.78.032305)

PACS number(s): 03.67.Mn, 42.50.Pq, 42.81.Qb

I. INTRODUCTION

Entanglement is one of the most striking features of quantum mechanics. Entangled states of two or more particles not only provide opportunities to test quantum nonlocality [1–3], but also have practical applications in many quantum information processes, including quantum teleportation, quantum cryptography, quantum computers, etc. [4–11]. Over the past few years, a large number of schemes have been proposed for generating entangled state in various quantum systems [12–19], which including semiconductor quantum dots (SCQDs) [15], cavity quantum electrodynamics (CQED) [16], trapped ions [18], and so on. Among these quantum systems, CQED system is always favored because of its low decoherent rate [16] and have many advantages in entanglement engineering [20]. In context of CQED, two-particle entangled states have been experimentally realized with Rydberg atoms crossing a nonresonant cavity [21].

Recently, it has been demonstrated that the high-dimensional entanglement can enhance the violations of local realism [22] and the security of quantum cryptography [23]. So, extensive research has been devoted to the generation high-dimensional entangled states of photons [24,25] and atoms [26,27] in recent years. Specifically, Mair *et al.* realized experimentally the high-dimensional entangled states of photons based on the spatial modes of the electromagnetic field carrying orbital angular momentum [24]. They showed that their schemes can be used to define an infinitely dimensional discrete Hilbert space. Subsequently, two CQED schemes were proposed for generating high-dimensional entangled states of atoms with a nonresonant cavity by cavity-assisted collisions [26] and an additional strong classical driven field [27], respectively. However, the collisions of the atoms were experienced in one nonresonant cavity, which requires high experimental techniques and has

a limited application in real quantum information processing.

Alternatively, entanglement between two spatially separated subsystems also is very useful for distributed quantum computation. So, people also began to study the two-dimensional (2D) and 3D entanglement between atoms trapped in distant optical cavities, through detection of leaking photons [28–30] or through direct linking of the cavities [31–37], in recent years. In particular, Feng *et al.* [28] proposed a scheme for generating 2D entangled state of two Λ -type atoms individually trapped in spatially separated cavities via the interference effects of polarized photons. However, it is a probabilistic scheme as it depends on the detection of the photons decaying from two leaking cavities and thus high efficient photon detectors are required. Subsequently, based on the cavity-fiber-cavity system, Zheng [37] *et al.* proposed a scheme for deterministically generating 3D entangled state of two spatially separated atoms through adiabatic passage along dark states. In this schemes, appropriate pulse sequence of cavity field and classical field are necessary for satisfying the conditions of dark-state evolution. Summing up the previous schemes, it is noticed that most of them are based on the resonant atom-field interaction.

In this paper, we proposed an alternative scheme for deterministically generating 3D entangled state of two distant five-level atoms based on the dispersive atom-field interaction. In the present protocol, we can adiabatically eliminate the excited states of atoms via choosing large enough frequency detuning of the atom field. So, the influence of atomic spontaneous decay on the fidelity of realizing entangled state can be suppressed effectively. In addition, our numerical simulation shows that the effect of photons leakage from fiber also can be suppressed effectively in the present scheme. As a result, the highly reliable 3D entangled state of two spatially separated atoms can be realized based on our proposed scheme.

The remainder of this paper is organized into four parts as follows. In Sec. II, we first describe the model under consid-

*xinyou_lv@163.com

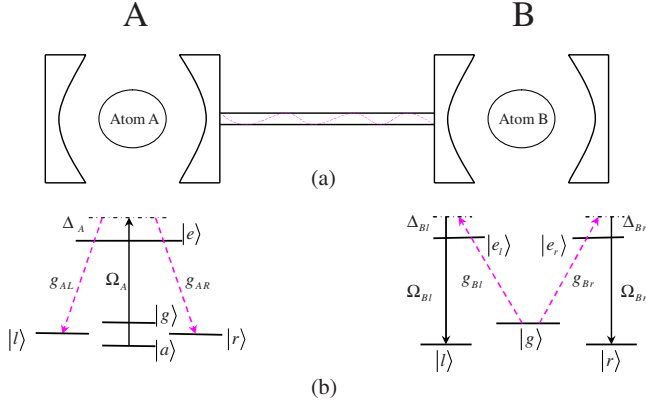


FIG. 1. (Color online) Two five-level atoms are trapped in two spatially separated double-mode cavities *A* and *B*, respectively. (a) The experimental setup. (b) The level configuration for each atom.

eration and then drive the effective Hamiltonian of system. In Sec. III, the generation of 3D atomic entangled state is provided and discussed. In Sec. IV, we demonstrate in detail the influences of atomic spontaneous decay, photon leakage out of the cavities and fiber on the generation of atomic entangled states. Finally, we conclude with a brief summary in Sec. V.

II. MODEL AND HAMILTONIAN

As shown in Fig. 1, we consider a cavity-fiber-cavity system, which consists of two double-mode cavities (cavities *A* and *B*) connected by an optical fiber. Two five-level atoms are individually trapped in the cavities *A* and *B*. In the cavity *A*, the atomic transition $|a\rangle_A \leftrightarrow |e\rangle_A$ (with resonant frequency ω_A^{ea}) is dispersively driven by a classical field with center frequencies ω_A ; the cavity modes a_{Ak} with frequencies ν_{Ak} ($k=l, r$) dispersively drive the atom transition $|e\rangle_A \leftrightarrow |k\rangle_A$ with resonant frequency ω_A^{ek} . In the cavity *B*, the atom transition $|e\rangle_B \leftrightarrow |k\rangle_B$ (with resonant frequency ω_B^{ek}) is dispersively driven by the classical field with center frequencies ω_{Bk} ; the cavity modes a_{Bk} with frequencies ν_{Bk} dispersively drive the atom transition $|e\rangle_B \leftrightarrow |g\rangle_B$ with resonant frequency ω_B^{eg} . Δ_A and Δ_{Bk} are the corresponding single photon frequency detunings and satisfy corresponding two-photon resonance conditions

$$\nu_{Ak} - \omega_A^{ek} = \omega_A - \omega_A^{ea} = \Delta_A, \quad (1a)$$

$$\nu_{Bk} - \omega_B^{eg} = \omega_{Bk} - \omega_B^{ek} = \Delta_{Bk}. \quad (1b)$$

Then, under the dipole and rotating wave approximation, the interaction Hamiltonian of the atom-cavity can be written in the interaction picture as ($\hbar=1$) [42,43]

$$H_I^{ac} = \sum_{k=l,r} [-\Delta_A |e\rangle_A \langle e| - \Delta_{Bk} |e_k\rangle_B \langle e_k| + (\Omega_A |e\rangle_A \langle a| + g_{Ak} a_{Ak} |e\rangle_A \langle k| + \Omega_{Bk} |e_k\rangle_B \langle k| + g_{Bk} a_{Bk} |e_k\rangle_B \langle g| + \text{H.c.})], \quad (2)$$

where the symbol H.c. means Hermitian conjugate; a_{Ak}^\dagger , a_{Bk}^\dagger

and a_{Ak} , a_{Bk} are the creation and annihilation operators for photons with polarization k ($k=l, r$ corresponding to left and right circular polarizations, respectively) associating with the corresponding quantized cavity modes. Ω_A , Ω_{Bk} and g_{Ak} , g_{Bk} denote the one-half Rabi frequencies and atom-field coupling constants, respectively. They are assumed to be real number in this paper, without loss generality.

By applying standard quantum optical techniques [38], under the large-detuning condition, i.e., $|\Delta_A|, |\Delta_{Bk}| \gg |\Omega_A|, |\Omega_{Bk}|, |g_{Ak}|, |g_{Bk}|$, the excited states of atoms $|e\rangle_A$, $|e_k\rangle_B$ are only virtually excited in the process of atom-field interaction. So, we can adiabatically eliminate the excited states of atoms and obtain the effective Hamiltonian [32,39–41]

$$H_{\text{eff1}}^{ac} = \sum_{k=l,r} \left[\frac{g_{Ak}^2}{\Delta_A} a_{Ak}^\dagger a_{Ak} |k\rangle_A \langle k| + \frac{\Omega_A^2}{\Delta_A} |a\rangle_A \langle a| + \frac{g_{Bk}^2}{\Delta_{Bk}} a_{Bk}^\dagger a_{Bk} |g\rangle_B \langle g| + \frac{\Omega_{Bk}^2}{\Delta_{Bk}} |k\rangle_B \langle k| + \left(\frac{g_{Ak} \Omega_A}{\Delta_A} a_{Ak}^\dagger |k\rangle_A \langle a| + \frac{\Omega_{Bk} g_{Bk}}{\Delta_{Bk}} a_{Bk} |k\rangle_B \langle g| + \text{H.c.} \right) \right], \quad (3)$$

where the first four terms represent cavity- and laser-induced atomic level shifts. The last two terms correspond to the effective Raman couplings. According to Ref. [39], the terms of cavity- and laser-induced atomic level shifts can be compensated for quite straightforwardly by using corresponding second lasers which couple corresponding atomic levels $|a\rangle_A$, $|k\rangle_A$ and $|g\rangle_B$, $|k\rangle_B$ nonresonantly with additional levels farther up in the atomic level scheme. Then, the effective Hamiltonian can be further reduced as

$$H_{\text{eff2}}^{ac} = \sum_{k=l,r} (\Omega_{eA}^k a_{Ak}^\dagger |k\rangle_A \langle a| + \Omega_{eB}^k a_{Bk} |k\rangle_B \langle g| + \text{H.c.}), \quad (4)$$

where $\Omega_{eA}^k = \frac{g_{Ak} \Omega_A}{\Delta_A}$ and $\Omega_{eB}^k = \frac{g_{Bk} \Omega_{Bk}}{\Delta_{Bk}}$ are the effective Rabi frequencies for the corresponding Raman transitions $|a\rangle_A \rightarrow |e\rangle_A \rightarrow |k\rangle_A$ and $|g\rangle_B \rightarrow |e_k\rangle_B \rightarrow |k\rangle_B$, respectively.

On the other hand, in the short fiber limit $(2L\bar{\nu})/(2\pi c) \ll 1$, where L is the length of fiber and $\bar{\nu}$ is the decay rate of the cavity field into a continuum of fiber modes, only the resonant mode of the fiber will interact with the cavity modes. For this case, the interaction Hamiltonian of cavity-fiber can be written as [33,34]

$$H_I^{cf} = \sum_{k=l,r} [\eta_k b_k (a_{Ak}^\dagger + a_{Bk}^\dagger) + \text{H.c.}], \quad (5)$$

where b_k is the annihilation operator of resonant mode of the fiber; η_k denotes the corresponding coupling strength.

Then, in the interaction picture, the total Hamiltonian of this cavity-fiber-cavity system is given by

$$H_I = H_{\text{eff2}}^{ac} + H_I^{cf} = \sum_{k=l,r} [\Omega_{eA}^k a_{Ak}^\dagger |k\rangle_A \langle a| + \Omega_{eB}^k a_{Bk} |k\rangle_B \langle g| + \eta_k b_k (a_{Ak}^\dagger + a_{Bk}^\dagger) + \text{H.c.}]. \quad (6)$$

III. 3D ENTANGLEMENT OF TWO ATOMS

In this section, we begin to study the generation of 3D entanglement between two spatially separated five-level atoms. First, we will show that the 3D entangled state of atoms $|\Psi_e\rangle = (|l\rangle_A |l\rangle_B + |g\rangle_A |g\rangle_B + |r\rangle_A |r\rangle_B) / \sqrt{3}$ can be deterministically generated in an ideal situation.

Consider that the atom A is prepared in the superposition state $(\sqrt{2}|a\rangle_A + |g\rangle_A) / \sqrt{3}$, atom B in the state $|g\rangle_B$, and all the field modes in vacuum state $|00\rangle_c |0\rangle_f$ at the initial time. Then, the initial state of system $|\psi(0)\rangle$ is the coherent superposition state $\frac{1}{\sqrt{3}}(\sqrt{2}|a\rangle_A |g\rangle_B + |g\rangle_A |g\rangle_B) |00\rangle_c |0\rangle_f$. When $|\psi(0)\rangle = |a\rangle_A |g\rangle_B |00\rangle_c |0\rangle_f$, the system state will evolve in the domination of the Schrödinger equation ($\hbar=1$)

$$i \frac{\partial}{\partial t} |\psi(t)\rangle = H_I |\psi(t)\rangle, \quad (7)$$

where H_I is given by the Hamiltonian (6), and $|\psi(t)\rangle$ denotes the state of system at time t . $|\psi(t)\rangle$ can be expressed as $|\psi(t)\rangle = \sum_{i=1}^9 C_i |\phi_i\rangle$, where $|\phi_i\rangle$ compose the subspace of system evolution, and are defined, respectively, as

$$|\phi_1\rangle = |a\rangle_A |g\rangle_B |00\rangle_c |0\rangle_f, \quad (8a)$$

$$|\phi_2\rangle = |l\rangle_A |g\rangle_B |1l\rangle_c |0\rangle_f, \quad (8b)$$

$$|\phi_3\rangle = |l\rangle_A |g\rangle_B |00\rangle_c |1l\rangle_f, \quad (8c)$$

$$|\phi_4\rangle = |l\rangle_A |g\rangle_B |01l\rangle_c |0\rangle_f, \quad (8d)$$

$$|\phi_5\rangle = |l\rangle_A |l\rangle_B |00\rangle_c |0\rangle_f, \quad (8e)$$

$$|\phi_6\rangle = |r\rangle_A |g\rangle_B |1r\rangle_c |0\rangle_f, \quad (8f)$$

$$|\phi_7\rangle = |r\rangle_A |g\rangle_B |00\rangle_c |1r\rangle_f, \quad (8g)$$

$$|\phi_8\rangle = |r\rangle_A |g\rangle_B |01r\rangle_c |0\rangle_f, \quad (8h)$$

$$|\phi_9\rangle = |r\rangle_A |r\rangle_B |00\rangle_c |0\rangle_f, \quad (8i)$$

where n_A , n_B , and n_f in $|n_A n_B\rangle_c |n_f\rangle$ denote the photon numbers in the cavity A , cavity B , and fiber, respectively. Associating with the Eqs. (7) and (8), we can get the expressions of coefficient C_i ,

$$C_1 = \frac{1}{2} \cos(\sqrt{2}\Omega_{eA}t) + \frac{\eta^2 + \Omega_{eA}^2 \cos(\sqrt{2\Omega_{eA}^2 + 2\eta^2}t)}{2(\Omega_{eA}^2 + \eta^2)}, \quad (9a)$$

$$C_2 = C_6 = -\frac{i}{2\sqrt{2}} \left[\sin(\sqrt{2}\Omega_{eA}t) + \frac{\Omega_{eA}}{\sqrt{\Omega_{eA}^2 + \eta^2}} \sin(\sqrt{2\Omega_{eA}^2 + 2\eta^2}t) \right], \quad (9b)$$

$$C_3 = C_7 = \frac{\eta\Omega_{eA}}{2(\Omega_{eA}^2 + \eta^2)} [\cos(\sqrt{2\Omega_{eA}^2 + 2\eta^2}t) - 1], \quad (9c)$$

$$C_4 = C_8 = \frac{i}{2\sqrt{2}} \left[\sin(\sqrt{2}\Omega_{eA}t) - \frac{\Omega_{eA}}{\sqrt{\Omega_{eA}^2 + \eta^2}} \sin(\sqrt{2\Omega_{eA}^2 + 2\eta^2}t) \right], \quad (9d)$$

$$C_5 = C_9 = \frac{1}{2\sqrt{2}(\Omega_{eA}^2 + \eta^2)} [\eta^2 + \Omega_{eA}^2 \cos(\sqrt{2\Omega_{eA}^2 + 2\eta^2}t) - (\Omega_{eA}^2 + \eta^2) \cos(\sqrt{2}\Omega_{eA}t)]. \quad (9e)$$

It should be pointed out that we have set $\Omega_{eA}^l = \Omega_{eA}^r = \Omega_{eA}$, $\Omega_{eB}^l = \Omega_{eB}^r = \Omega_{eB} = \sqrt{2}\Omega_{eA}$ and $\eta_l = \eta_r = \eta$ in the above calculation. From the above equations, we notice that the state of system will evolve into the state $|\psi(t)\rangle = \frac{1}{\sqrt{2}}(|l\rangle_A |l\rangle_B + |r\rangle_A |r\rangle_B) |00\rangle_c |0\rangle_f$ (corresponding to $C_5 = C_9 = 1/\sqrt{2}$, $C_1 = C_2 = C_3 = C_4 = C_6 = C_7 = C_8 = 0$), when $t = \frac{m\pi}{\sqrt{2}\Omega_{eA}}$ ($m=1, 3, 5, \dots$), $\eta = \sqrt{n^2 - 1}\Omega_{eA}$ ($n=2, 4, 6, \dots$), for the initial condition $|\psi(0)\rangle = |a\rangle_A |g\rangle_B |00\rangle_c |0\rangle_f$.

On the other hand, when $|\psi(0)\rangle = |g\rangle_A |g\rangle_B |00\rangle_c |0\rangle_f$, the system state will remain unchanged along with the evolution of time. So, the system will evolve into the state $|\Psi_e\rangle |00\rangle_c |0\rangle_f$ under appropriate conditions, when $|\psi(0)\rangle = \frac{1}{\sqrt{3}}(\sqrt{2}|a\rangle_A |g\rangle_B + |g\rangle_A |g\rangle_B) |00\rangle_c |0\rangle_f$. The state $|\Psi_e\rangle |00\rangle_c |0\rangle_f = \frac{1}{\sqrt{3}}(|l\rangle_A |l\rangle_B + |g\rangle_A |g\rangle_B + |r\rangle_A |r\rangle_B) |00\rangle_c |0\rangle_f$ is a product state of the 3D entangled state of atoms and the vacuum state of cavity modes and fiber mode, and hence we get the 3D entangled state of two spatially separated atoms $|\Psi_e\rangle$, which is completely separated from the cavity fields and fiber modes.

Summing up the discussion above, it is noticed that the 3D entangled state, $|\Psi_e\rangle$ can be deterministically generated in an ideal situation, which includes $\Omega_{eB} = \sqrt{2}\Omega_{eA}$. However, there are usually some deviation of the ratio coefficient between two effective Rabi frequencies from the value $\sqrt{2}$ in practical situations. In order to study the influence of this deviation on the fidelity F_e of realizing atomic entangled state, we present the two-dimensional plot of the dependence of F_e on time $\Omega_{eA}t$ for different ratio coefficient s , as shown in Fig. 2. The fidelity F_e is defined as $F_e = |\langle \Psi_e | \langle 00 | \langle 00 | \langle \Psi_e | \psi(t) \rangle|^2$ and the ratio coefficient s satisfies the relationship $\Omega_{eB} = s\Omega_{eA}$. It is clearly shown from Fig. 2 that the F_e is highly stable to the deviation of the ratio coefficient s from the condition $s = \sqrt{2} \approx 1.414$, with which the 3D atomic entangled state can be realized determinately. As a result, based on our scheme, the 3D atomic entangled state $|\Psi_e\rangle$ also can be realized with high fidelity, even that the ideal condition $\Omega_{eB} = \sqrt{2}\Omega_{eA}$ could not be satisfied accurately in practical situations.

In the present scheme, $\eta = \sqrt{n^2 - 1}\Omega_{eA}$ ($n=2, 4, 6, \dots$) is another necessary condition for deterministically generating 3D entangled state $|\Psi_e\rangle$. However, it is noticed from Eqs. (9a)–(9d) that this condition can be neglected approximately when $\eta \gg \Omega_{eA}$. For seeing this more clearly, we give the effects of coupling strength η on the fidelity of realizing the 3D entangled state $|\Psi_e\rangle$, as shown in Fig. 3. It is shown from Fig. 3 that the fidelity F_e becomes more and more stable to the coupling strength η along with its increase. More specifically, the maximum value of F_e is 1 and

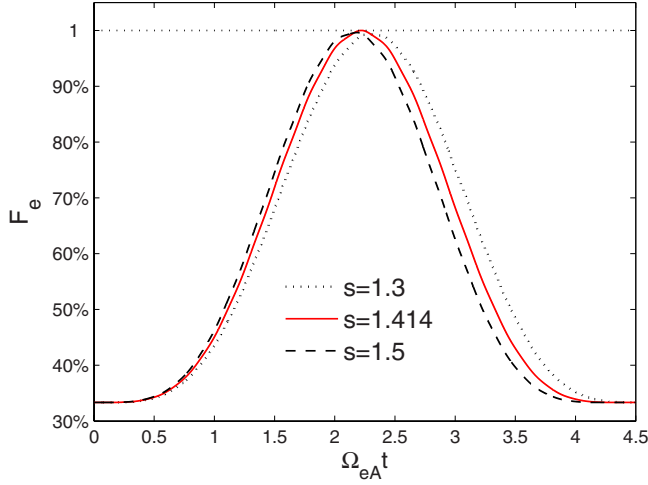


FIG. 2. (Color online) The fidelity F_e for realizing the 3D entangled state $|\Psi_e\rangle$ versus time $\Omega_{eA}t$ for different s .

its minimum value is also larger than 99.7%, when the coupling strength $\eta \geq 20\Omega_{eA}$. As a result, the condition $\eta = \sqrt{n^2 - 1}\Omega_{eA}$ ($n=2, 4, 6, \dots$) for deterministically realizing 3D entangled state of atoms can be neglected approximately when $\eta \geq 20\Omega_{eA}$ in our scheme.

Before ending this section, let us qualitatively explain the process of generating 3D entanglement of atoms based on our scheme. Consider that at the initial time the atom A is in the state $|a\rangle_A$, atom B in the state $|g\rangle_B$, and all the field modes in vacuum state $|00\rangle_c|0\rangle_f$. First, the atom A will go through the transition $|a\rangle_A \xrightarrow{\Omega_A} |e\rangle_A \xrightarrow{a_{Al}^\dagger} |l\rangle_A$ (or $|a\rangle_A \xrightarrow{\Omega_A} |e\rangle_A \xrightarrow{a_{Ar}^\dagger} |r\rangle_A$), and emit a left (or right) circular polarization photon into the cavity A , respectively. Through the fiber, the left (or right) circular polarization photon will enter into cavity B . Then, the atom B will absorb the left (or right) circular polarization photon and go through the transition $|g\rangle_B \xrightarrow{\Omega_B} |e\rangle_B \xrightarrow{b_{Bl}^\dagger} |l\rangle_B$ (or $|a\rangle_B \xrightarrow{\Omega_B} |e\rangle_B \xrightarrow{b_{Br}^\dagger} |r\rangle_B$). On the other hand, when atom A is initially in

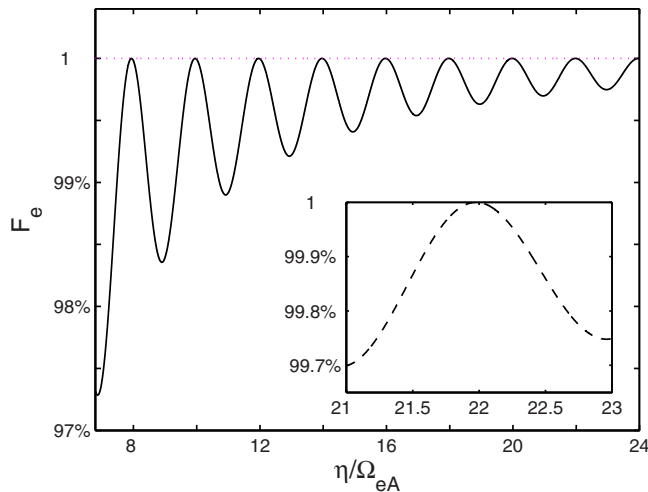


FIG. 3. (Color online) The fidelity F_e of realizing the extremely entangled state $|\Psi_e\rangle$ versus coupling strength η when $t = \frac{\pi}{\sqrt{2}\Omega_{eA}}$, $\Omega_{eB} = \sqrt{2}\Omega_{eA}$.

the state $|g\rangle_A$, atom B in $|g\rangle_B$, and all the field modes in vacuum state $|00\rangle_c|0\rangle_f$, the state of atoms will remain unchanged. So, the 3D entangled state $|\Psi_e\rangle = (|l\rangle_A|l\rangle_B + |g\rangle_A|g\rangle_B + |r\rangle_A|r\rangle_B)/\sqrt{3}$ can be generated when atoms A and B are initially in the coherent superposition state $(\sqrt{2}|a\rangle_A|g\rangle_B + |g\rangle_A|g\rangle_B)/\sqrt{3}$, and all the field modes in vacuum state $|00\rangle_c|0\rangle_f$.

IV. EFFECTS OF ATOMIC SPONTANEOUS DECAY AND PHOTON LEAKAGE

In this section, we will study the influences of atomic spontaneous decay and photon leakage out of the cavities and fiber on the generation of 3D atomic entangled state $|\Psi_e\rangle$. Using the density-matrix formalism, the master equation for the density matrix of whole system can be expressed as

$$\begin{aligned} \dot{\rho} = & -i[H_I^{ac} + H_I^{cf}, \rho] - \sum_{k=l,r} \left[\frac{\gamma_{fk}}{2} (b_k^\dagger b_k \rho - 2b_k \rho b_k^\dagger + \rho b_k^\dagger b_k) \right. \\ & - \sum_{i=A,B} \frac{\Gamma_{ik}}{2} (a_{ik}^\dagger a_{ik} \rho - 2a_{ik} \rho a_{ik}^\dagger + \rho a_{ik}^\dagger a_{ik}) \left. \right] \\ & - \sum_{j=a,l,r} \frac{\gamma_{Aa}^j}{2} (\sigma_{ec}^A \rho - 2\sigma_{je}^A \rho \sigma_{ej}^A + \rho \sigma_{ee}^A) \\ & - \sum_{k=l,r} \sum_{j=k,g} \frac{\gamma_{Ba}^{kj}}{2} (\sigma_{e_k e_k}^B \rho - 2\sigma_{je_k}^B \rho \sigma_{e_k j}^B + \rho \sigma_{e_k e_k}^B), \end{aligned} \quad (10)$$

where H_I^{ac} and H_I^{cf} are given by Eqs. (2) and (5), respectively; γ_{Aa}^j and γ_{Ba}^{kj} denote the spontaneous decay rates of atoms from level $|e\rangle_A$ to $|j\rangle_A$ and $|e_k\rangle_B$ to $|j\rangle_B$, respectively; Γ_{ik} and γ_{fk} denote the decay rates of cavity fields and fiber modes, respectively; $\sigma_{mn}^i = |m\rangle_i \langle n|$ ($m, n = e, e_k, j$) are the usual Pauli matrices. By solving numerically Eq. (10) in the subspace spanned by the basis vectors (8) and $|\phi_{10}\rangle = |e\rangle_A|g\rangle_B|00\rangle_c|0\rangle_f$, $|\phi_{11}\rangle = |l\rangle_A|e\rangle_B|00\rangle_c|0\rangle_f$, $|\phi_{12}\rangle = |r\rangle_A|e\rangle_B|00\rangle_c|0\rangle_f$, we present the effects of the decay rates γ_a ($\gamma_a = \sum_{j=a,l,r} \gamma_{Aa}^j = \sum_{j=g,l} \gamma_{Ba}^{jl} = \sum_{j=g,r} \gamma_{Ba}^{rj}$), Γ and γ_f on the fidelity F_e of generating atomic entangled state $|\Psi_e\rangle$, as shown in Fig. 4. In the calculation, for simplicity all involving parameters are reduced to dimensionless units by scaling γ and chosen $\gamma_{Aa}^a = \gamma_{Aa}^{ek} = \gamma_a/3$ ($k=l,r$), $\gamma_{Ba}^{kg} = \gamma_{Ba}^{ek} = \gamma_a/2$, $\Gamma_{Ak} = \Gamma_{Bk} = \Gamma$, $\gamma_{fk} = \gamma_f$ without loss of generality. From Fig. 4, it is easy to find that the influences of decay rates γ_a , Γ , and γ_f on the fidelity F_e are very little when $\Gamma = \gamma_a = \gamma_f \leq 0.01\gamma$. Even when $\Gamma = \gamma_a = \gamma_f = 0.01\gamma$, the fidelity F_e still can be larger than 95%. In order to further explicitly show the influences of decay rates Γ , γ_a , and γ_f on F_e , respectively, we also plot the function curves for F_e versus Γ , γ_a , and γ_f in Fig. 5, when $\gamma t = 9.3$. Comparing the main part and inserted part of Figs. 5(a) and 5(b), we notice that the influences of atomic spontaneous decay rate γ_a and fiber decay rate γ_f on F_e are much smaller than that of cavity field decay rate Γ , and hence they can be safely neglected in our scheme. The above numerical results can be qualitatively explained as follows. Under the conditions $|\Delta_A|, |\Delta_{Bk}| \gg |\Omega_A|, |\Omega_{Bk}|, |g_{Ak}|, |g_{Bk}|$, and $|\eta| \gg |\Omega_{eA}|, |\Omega_{eB}|$, the atomic excited states $|e\rangle_A$, $|e\rangle_{Bk}$ and fiber

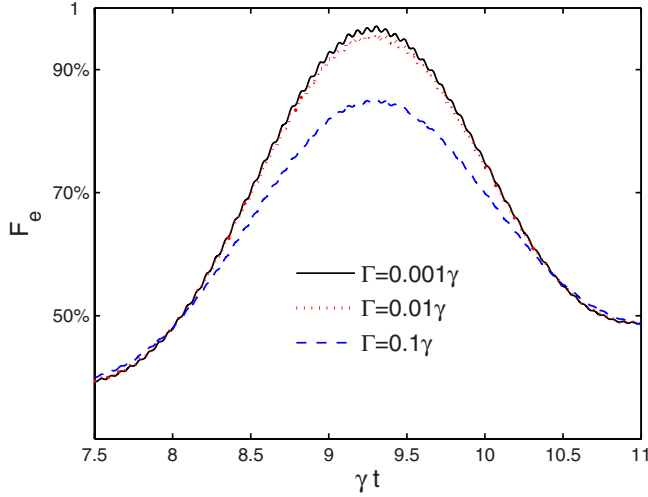


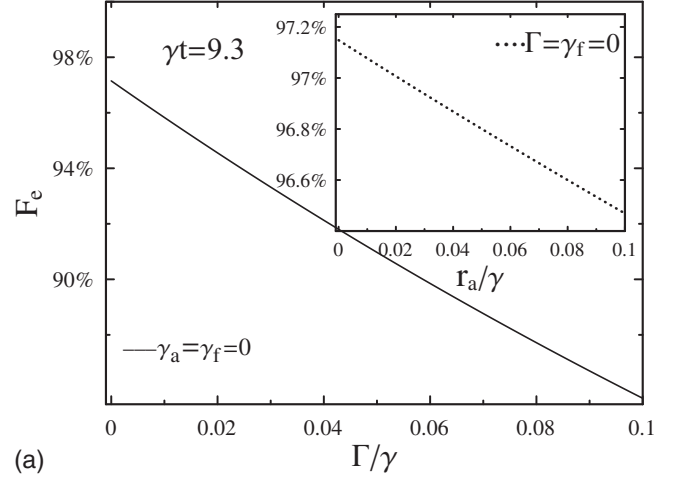
FIG. 4. (Color online) The fidelity F_e of realizing the 3D entangled state $|\Psi_e\rangle$ versus time γt for different decay rates Γ ($\gamma_a = \gamma_f = \Gamma$). The corresponding system parameters are chosen as $g_{A1} = g_{A2} = 10\gamma$, $g_{B1} = g_{B2} = 12.5\gamma$, $\Omega_A = 10\gamma$, $\Omega_{B1} = \Omega_{B2} = 10\gamma$, $\eta = 25\gamma$, and $\Delta_A = \Delta_{B1} = \Delta_{B2} = -100\gamma$.

mode b_k are only virtually excited in the whole interaction process, and hence the effects of atomic decay rate γ_a and fiber decay rate γ_f are suppressed strongly when $|\Delta_A|, |\Delta_{Bk}| \approx 10|\Omega_A|, |\Omega_{Bk}|, |g_{Ak}|, |g_{Bk}|$, and $|\eta| \approx 25|\Omega_{eA}|, |\Omega_{eB}|$, as shown in Fig. 5. It is also shown from Fig. 5 that properly low decay rate ($\Gamma \leq 0.02\gamma$) of cavity field is still needed for getting atomic entangled state with high fidelity ($F_e \geq 94\%$) in our scheme.

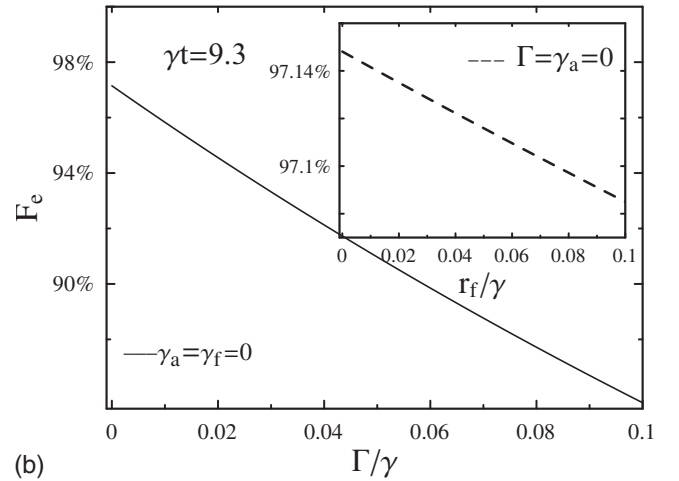
Before ending this section, let us briefly discuss the experimental feasibility of our scheme. First, the two five-level atoms can be realized by choosing the hyperfine-split levels for the D lines of cold alkali-metal atoms [44,45]. For instance, in the case of the cesium atom with nuclear spin $I = 7/2$, according to the selective rule of photon absorption and emission, the levels of atoms and polarizations of cavity fields and classical fields can be chosen as shown in Fig. 6. Secondly, based on the recent experiments about realizing high- Q cavity and strong atom-cavity coupling [46], we can choose $g_{A1}/2\pi = g_{A2}/2\pi \approx 750$ MHz, $\Delta_A/2\pi = \Delta_{B1}/2\pi = \Delta_{B2}/2\pi \approx -7.5$ GHz, $\gamma_a/2\pi = \gamma_f/2\pi \approx 7.5$ MHz, $\Gamma/2\pi \approx 1.5$ MHz (corresponding to the cavity quality factor $Q \sim 10^8$) as the basal system parameters of our scheme. Then, the condition $\Gamma \leq 0.02\gamma$ that is necessary for realizing 3D atomic entangled state with high fidelity, can be satisfied with these system parameters. Lastly, along with the progress of fiber-cavity coupling techniques [47,48], we believe that the 3D entanglement of atoms with high fidelity can be realized based on our scheme.

V. CONCLUSION

In conclusion, based on the dispersive atom-field interaction, we have proposed a scheme for deterministically generating 3D entanglement between two spatially separated five-level atoms in an ideal situation. In this scheme, the atomic spontaneous decay and photon leakage out of the



(a)



(b)

FIG. 5. The fidelity F_e of realizing the 3D entangled state $|\Psi_e\rangle$ versus Γ and γ_a [panel (a)] and versus Γ and γ_f [panel (b)] when $\gamma t = 9.3$. The other system parameters are same as in Fig. 4.

fiber can be efficiently suppressed, since the excited states of atoms and fiber mode are only virtually excited in the whole interaction process. We also show that this scheme is highly stable to the deviation of the ratio coefficient between two effective Rabi frequencies from that in the ideal situation. Lastly, the experimental feasibility of our scheme is discussed and as a result, the present scheme is considered as a promising scheme for realizing entanglement with high fidelity.

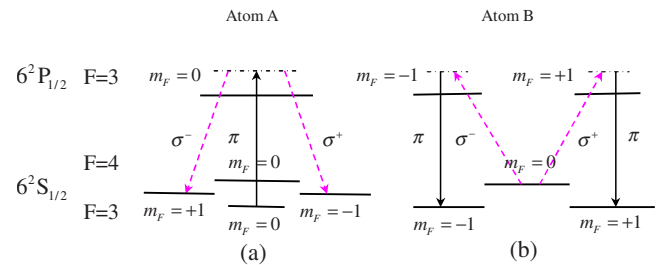


FIG. 6. (Color online) The five-level schemes of atom A [panel (a)] and atom B [panel (b)]. σ^- , σ^+ , and π denote left, right circular, and line polarizations light, respectively.

ACKNOWLEDGMENTS

The research is supported in part by the Natural Science Foundation of China (Grant Nos. 10575040, 90503010,

10634060, and 10747133) and by the National Basic Research Program of China under Contract No. 2005CB724508. We would like to thank Professor Ying Wu for helpful discussions and encouragement.

-
- [1] A. Einstein, B. Podolsky, and N. Rosen, *Phys. Rev.* **47**, 777 (1935).
- [2] J. S. Bell, *Physics* (Long Island City, N.Y.) **1**, 195 (1965).
- [3] D. M. Greenberger, M. Horne, A. Shimony, and A. Zeilinger, *Am. J. Phys.* **58**, 1131 (1990).
- [4] M. A. Nielsen and I. L. Chuang, *Quantum Computation and Quantum Information* (Cambridge University Press, Cambridge, 2000).
- [5] C. H. Bennett, G. Brassard, C. Crepeau, R. Jozsa, A. Peres, and W. K. Wootters, *Phys. Rev. Lett.* **70**, 1895 (1993); C. H. Bennett and D. P. DiVincenzo, *Nature* (London) **404**, 247 (2000).
- [6] D. P. Divincenzo, *Science* **270**, 225 (1995).
- [7] D. Bouwmeester, J. W. Pan, K. Mattle, M. Eibl, H. Weinfurter, and A. Zeilinger, *Nature* (London) **390**, 575 (1997).
- [8] R. Prevedel, M. Aspelmeyer, C. Brukner, A. Zeilinger, and T. D. Jennewein, *J. Opt. Soc. Am. B* **24**, 241 (2007).
- [9] A. K. Ekert, *Phys. Rev. Lett.* **67**, 661 (1991).
- [10] A. Barenco, D. Deutsch, A. Ekert, and R. Jozsa, *Phys. Rev. Lett.* **74**, 4083 (1995).
- [11] W.-X. Yang, Z.-M. Zhan, and J.-H. Li, *Phys. Rev. A* **72**, 062108 (2005); W.-X. Yang, Z.-X. Gong, W.-B. Li, and X.-X. Yang, *J. Phys. A* **40**, 155 (2007).
- [12] I. L. Chuang and Y. Yamamoto, *Phys. Rev. A* **52**, 3489 (1995).
- [13] G.-X. Li, H. T. Tan, and M. Macovei, *Phys. Rev. A* **76**, 053827 (2007).
- [14] Xin-You Lü, Ji-Bing Liu, Liu-Gang Si, and Xiaoxue Yang, *J. Phys. B* **41**, 035501 (2008); Xin-You Lü, Ji-Bing Liu, Yü Tian, Pei-Jun Song, and Zhi-Ming Zhan, *Europhys. Lett.* **82**, 64003 (2008).
- [15] J. H. Reina, L. Quiroga, and N. F. Johnson, *Phys. Rev. A* **62**, 012305 (2000).
- [16] T. Pellizzari, S. A. Gardiner, J. I. Cirac, and P. Zoller, *Phys. Rev. Lett.* **75**, 3788 (1995).
- [17] Y. Wu, K. W. Chan, M. C. Chu, and P. T. Leung, *Phys. Rev. A* **59**, 1662 (1999).
- [18] Q. A. Turchette, C. S. Wood, B. E. King, C. J. Myatt, D. Leibfried, W. M. Itano, C. Monroe, and D. J. Wineland, *Phys. Rev. Lett.* **81**, 3631 (1998).
- [19] J. I. Cirac and P. Zoller, *Phys. Rev. Lett.* **74**, 4091 (1995).
- [20] J. M. Raimond, M. Brune, and S. Haroche, *Rev. Mod. Phys.* **73**, 565 (2001); H. Mabuchi and A. C. Doherty, *Science* **298**, 1372 (2002).
- [21] S. Osnaghi, P. Bertet, A. Auffeves, P. Maioli, M. Brune, J. M. Raimond, and S. Haroche, *Phys. Rev. Lett.* **87**, 037902 (2001).
- [22] D. Kaszlikowski, P. Gnacinski, M. Zukowski, W. Miklaszewski, and A. Zeilinger, *Phys. Rev. Lett.* **85**, 4418 (2000).
- [23] M. Bourennane, A. Karlsson, and G. Björk, *Phys. Rev. A* **64**, 012306 (2001); D. Bruss and C. Macchiavello, *Phys. Rev. Lett.* **88**, 127901 (2002); N. J. Cerf, M. Bourennane, A. Karlsson, and N. Gisin, *Phys. Rev. Lett.* **88**, 127902 (2002).
- [24] A. Mair, A. Vaziri, G. Weihs, and A. Zeilinger, *Nature* (London) **412**, 313 (2001).
- [25] A. Lamas-Linares, J. C. Howell, and D. Bouwmeester, *Nature* (London) **412**, 887 (2001); J. C. Howell, A. Lamas-Linares, and D. Bouwmeester, *Phys. Rev. Lett.* **88**, 030401 (2002).
- [26] X. B. Zou, K. Pahlke, and W. Mathis, *Phys. Rev. A* **67**, 044301 (2003).
- [27] S. B. Zheng, *Phys. Rev. A* **68**, 035801 (2003).
- [28] X. L. Feng, Z. M. Zhang, X. D. Li, S. Q. Gong, and Z. Z. Xu, *Phys. Rev. Lett.* **90**, 217902 (2003).
- [29] D. E. Browne, M. B. Plenio, and S. F. Huelga, *Phys. Rev. Lett.* **91**, 067901 (2003).
- [30] L. M. Duan and H. J. Kimble, *Phys. Rev. Lett.* **90**, 253601 (2003).
- [31] J. I. Cirac, P. Zoller, H. J. Kimble, and H. Mabuchi, *Phys. Rev. Lett.* **78**, 3221 (1997).
- [32] S. Clark, A. Peng, M. Gu, and S. Parkins, *Phys. Rev. Lett.* **91**, 177901 (2003).
- [33] A. Serafini, S. Mancini, and S. Bose, *Phys. Rev. Lett.* **96**, 010503 (2006).
- [34] P. Peng and F. L. Li, *Phys. Rev. A* **75**, 062320 (2007).
- [35] L. B. Chen, M. Y. Ye, G. W. Lin, Q. H. Du, and X. M. Lin, *Phys. Rev. A* **76**, 062304 (2007).
- [36] Z. Q. Yin and F. L. Li, *Phys. Rev. A* **75**, 012324 (2007).
- [37] S. Y. Ye, Z. R. Zhong, and S. B. Zheng, *Phys. Rev. A* **77**, 014303 (2008).
- [38] C. W. Gardiner, *Quantum Noise* (Springer-Verlag, Berlin, 1991).
- [39] T. Pellizzari, *Phys. Rev. Lett.* **79**, 5242 (1997).
- [40] Y. Wu, *Phys. Rev. A* **54**, 1586 (1996).
- [41] Y. Wu and P. T. Leung, *Phys. Rev. A* **60**, 630 (1999).
- [42] M. O. Scully and M. S. Zubairy, *Quantum Optics* (Cambridge University Press, Cambridge, 1997) Chap. 14, p. 409.
- [43] Y. Wu, L. Wen, and Y. Zhu, *Opt. Lett.* **28**, 631 (2003).
- [44] D. A. Steck, <http://steck.us/alkalidata>
- [45] Y. Wu and X. Yang, *Phys. Rev. A* **70**, 053818 (2004).
- [46] S. M. Spillane, T. J. Kippenberg, K. J. Vahala, K. W. Goh, E. Wilcut, and H. J. Kimble, *Phys. Rev. A* **71**, 013817 (2005); J. R. Buck and H. J. Kimble, *ibid.* **67**, 033806 (2003); D. K. Armani, T. J. Kippenberg, S. M. Spillane, and K. J. Vahala, *Nature* (London) **421**, 925 (2003); D. W. Vernooy, V. S. Ilchenko, H. Mabuchi, E. W. Streed, and H. J. Kimble, *Opt. Lett.* **23**, 247 (1998).
- [47] S. M. Spillane, T. J. Kippenberg, O. J. Painter, and K. J. Vahala, *Phys. Rev. Lett.* **91**, 043902 (2003).
- [48] P. E. Barclay, K. Srinivasan, O. Painter, B. Lev, and H. Mabuchi, *Appl. Phys. Lett.* **89**, 131108 (2006).